

ELECTRIC SOLAR WIND SAIL CONTROL AND NAVIGATION

Petri Toivanen,* Pekka Janhunen, Jouni Envall, and Sini Merikallio

The electric solar wind sail is a propulsion system that uses long centrifugally spanned and electrically charged tethers to extract solar wind momentum for spacecraft thrust. The sail solar zenith angle and phase can be controlled by modulating the voltage of each tether separately to produce net torque for attitude control and thrust vectoring. In this paper, we cover the basics of the electric sail control based on our set of dynamical models including single tether simulation and rigid body and fully dynamical simulations for the entire sail. Short descriptions of these models are given. We also consider real solar wind conditions based on available solar wind data and address the effects of the solar wind density and velocity variations on the sail dynamics, control, and navigation.

INTRODUCTION

The electric sail is a propulsion concept to extract solar wind momentum for the spacecraft thrust.² It was motivated by so-called magnetic propulsion,¹¹ but instead of a magnetic field, it proposes an electric field created by a conducting light-weight wire mesh as an obstacle for the solar wind. The electric field and the associated positive charge was maintained by an electron gun powered by solar panels. Later, it was noticed that the electric obstacle can also be generated by a set of long centrifugally spread micro-meteoroid resistant tethers¹ rotating along with the spacecraft⁴ (Figure 1).

Presently, the sail configuration is such that the tips of the main radial charged tethers are connected to each other by non-conducting auxiliary tethers (Figure 1). At each of the tether tip, there is a light-weight remote unit hosting two reels for releasing the auxiliary tethers when the sail is deployed.⁵ Furthermore, the remote units also houses micro-thrusters to generate the required angular momentum of the fully set sail. Note that the amount of required delta-v is much less when thrusters are located at the tether tips than if the thrusters were located at the main spacecraft. These key components of such a design are presently developed in ESAIL project under the EU/FP7 program.

The electric sail thrust arises from the interaction of the solar wind and an electric potential structure of a few tens of kV. Since the projected voltage of a few tens of kV is much larger than that corresponding to the electron temperature, the traditional theory of Debye shielding is not necessarily valid as it assumes the contrary. This interaction was addressed by using a particle-in-cell simulation.³ It was concluded that the spatial scale size

*Research Scientist, Finnish Meteorological Institute, P.O. Box 503, FIN-00101, Helsinki, Finland

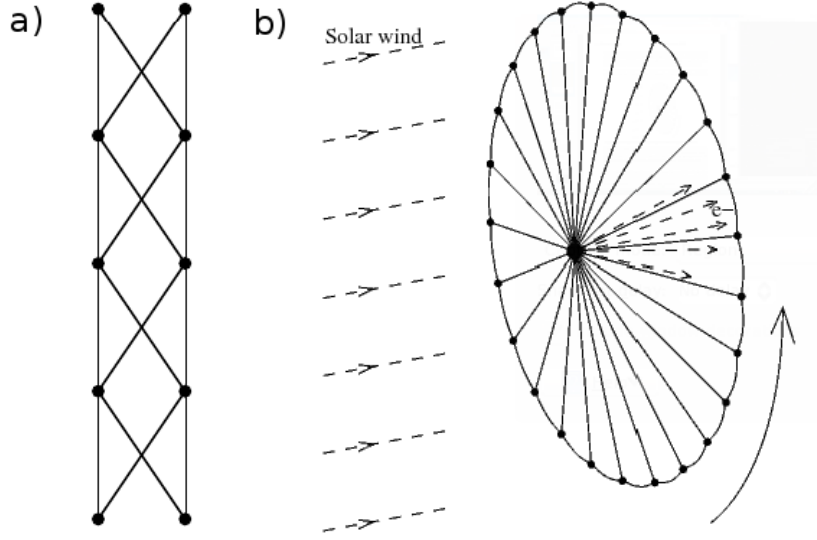


Figure 1. a) Micrometeoroid resistant main tether¹ and b) present sail design including remote units (black dots at the tips of the radial main tethers) and auxiliary tethers connecting the main tether tips.

of the electric barrier is of the order of a few hundreds of meters corresponding to a thrust of several hundreds of nN/m.³ The scale size is in good agreement with results published elsewhere.⁸ The amount of electron current collected by the positively charged tethers was also estimated and it obeys the orbital motion limited theory. The current is proportional to the electron number density.³ Given these values, 1-N thrust can be generated with a 100–200 kg propulsion system as a baseline sail.

In terms of the tether voltage V and the solar wind dynamic pressure P_{dyn} , the thrust per unit tether length was given⁵ as

$$\frac{dF_u}{dz} \approx 0.18 \max(0, V - V_w) \sqrt{\epsilon_0 P_{\text{dyn}}}. \quad (1)$$

The dynamic pressure, $P_{\text{dyn}} = m_p n_w u^2$ with n_w and u being the solar wind number density and flow speed, respectively. The electric potential V_w corresponds to the kinetic energy ($m_p u^2 / 2e$) of the solar wind ions. It is worthwhile to note that the thrust scales in radial distance r from the Sun as r^{-1} as $n_w \propto r^{-2}$ and $u \propto r^0$. Note, however, that the solar panel power requirement scales as r^{-2} as does the available solar radiation.

The direction of the electric sail force exerted on a single tether is depicted in Figure 2. It is aligned with and proportional to the solar wind component perpendicular to the tether. Depending on the sail angle α and the coning angle Λ , the magnitude and direction of the thrust varies in tether rotation phase. Thus it is obvious that active voltage modulation along with the sail rotation is required to nullify the exerted torque and to maintain the sail angle. Note that when the tether is aligned with Y_{SE} axis, the thrust is maximized and mostly in the solar wind direction. Taking this into account, the average force over the tether rotational phase is not perpendicular to the rotation plane (dotted line in Figure 2), i.e.,

the collective thrust is not perpendicular to the sail. This is a central difference to the solar photon sail, for which the thrust is always perpendicular to the sail if fully reflective solar sail material is assumed. It can also be noted that while the electric sail control algorithm can be anticipated to be analogous to that of a helicopter flight control, there is a crucial difference: for the helicopter, azimuthal and latitudinal motion of the blades are mostly decoupled since the lift to the blade is much larger than the drag.

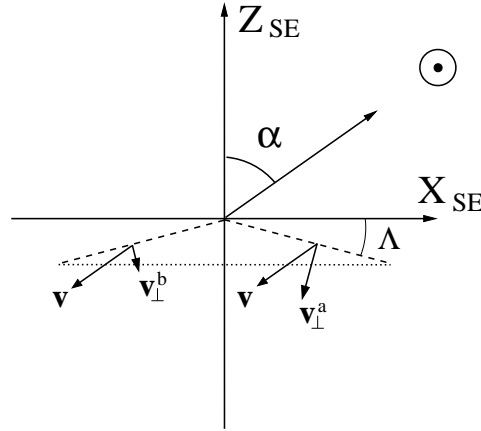


Figure 2. Sail ecliptic coordinates and minimum (v_{\perp}^b) and maximum (v_{\perp}^a) solar wind velocity components perpendicular to the tether.

SAIL DYNAMICAL MODELS

Model single tether dynamics

Concerning the electric sail control, there are several analytical rules that can be derived from a simplified tether model dynamics of a rotating rigid beam. Applying the thrust law of Equation (1), it has been shown that the tether forced by the solar wind dynamic pressure can be described as a spherical pendulum.¹⁰ Most importantly, it can be shown that such a voltage modulation exist that the tether rotation maintains any realistic rotation plane with respect to the sun direction. Since the sail is designed for some maximum tether voltage, this implies that a certain part of the voltage power has to be reserved for the sail control. An estimate for the voltage reserve, i.e., the sail efficiency can be obtained from the maximum value of the modulation expressed as

$$\max(g(\varphi)) = \frac{2(1 - \chi^2)^{5/2}}{(2 + \chi^2)(1 - |\chi|)^3} \quad (2)$$

where $\chi = \tan \alpha \tan \Lambda$.¹⁰ Figure 3a shows the efficiency as a function of coning angle for several sail angles. It can be concluded that the smaller the coning angle or the faster the sail spin is the more efficient the sail is. Furthermore, increasing the sail angle leads to a larger thrust component aligned with sail orbital velocity, but it also decreases the sail efficiency according to Figure 3a. Taking this into account, Figure 3b shows equicontours of the thrust component aligned with the sail orbital speed as a function of sail and coning

angles. For small sail angles, the thrust increases independently of the coning angle as expected, but for sail angles larger than about 20° , the thrust shows strong dependence on the coning angle, and the thrust levels start to decrease before the geometrical maximum at the sail angle of 45° is reached. It can be concluded that the larger the tensile strength of the tether material the faster sail rotation rates can be applied and the more efficient the sail is. Note that these considerations only hold for a sail consisting of mechanically uncoupled tethers, and the sail with auxiliary tethers as shown in Figure 1 presumably more efficient since all the tethers rotate in unison. Here, the tether azimuthal speed varies within the spin period, thus requiring voltage reserve for the control and the efficiency is reduced.

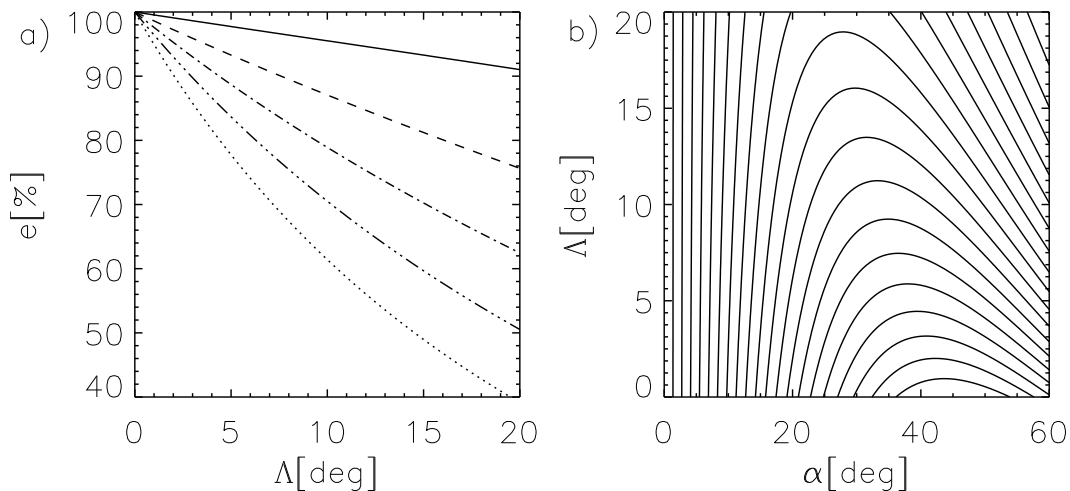


Figure 3. Sail efficiency as a function of coning angle for five sail angles of 5° , 15° , 25° , 35° , and 45° .

Another central result is associated with the sail rotation plane maneuvers in terms of the turning of the sail angle. Since the modulation causes variations in the tether angular velocity, it can be anticipated that the sail rotation rate is enhanced when the sail is turned. Figure 4 shows the coning angle and the spin rate as functions of sail turning angle. For example, considering a case that the sail rotation is initiated at $\alpha = 0$, after turning of the sail to 45 degrees, the spin rate is enhanced by the factor of about 1.5. This implies also that a considerable fraction of the sail angular momentum can be generated while turning the sail which reduces the requirements of the system generating the initial angular momentum.

The enhancement of the sail rotation under sail angle turning implies an intriguing effect to be taken into account when designing electric sail control and missions. The sail has to be actively turned while orbiting the Sun to maintain the designed sail angle. In other words, a small correction has to be included in the tether modulation to account for the orbital Coriolis effect. Based on the simple dynamical model, it has been shown that the angular frequency ω varies as

$$\omega = \omega_0 e^{\Omega \tan \alpha (t-t_0)} \quad (3)$$

as a function of time (t), where Ω is the angular frequency corresponding to the spacecraft orbiting the Sun, about $1^\circ/\text{yr}$ for 1 AU.¹⁰ The rotation rate is either decreased or increased

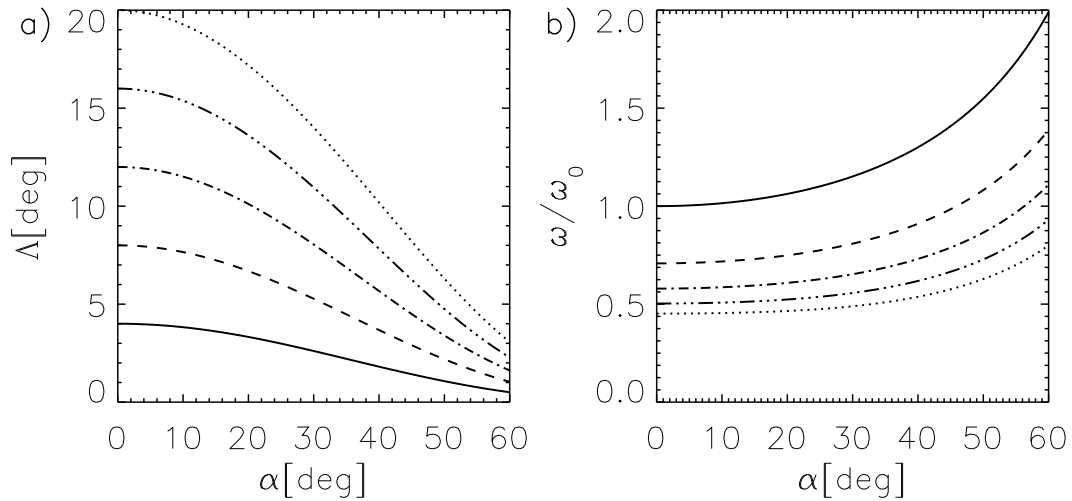


Figure 4. a) Coning angle and b) relative tether spin rate as a function of the sail turning angle α for five initial coning angles of 4° , 8° , 12° , 16° , and 20° . The spin rate is scaled to the initial spin rate for the coning angle of 4° .

depending on the sail angle, i.e., whether the sail is spiralling inward or outward from the Sun, respectively.

Fully dynamical model

The fully dynamical simulation code was developed to address the following key concerns in dynamics of the electric sail: Identification of mechanically stable flight configurations; Deployment of the sail; and Emergency scenarios such as sudden tether cut. It includes self-consistent mechanical interactions between the main spacecraft, main tethers, auxiliary tethers, and remote units. The spacecraft and remote units are described as rigid bodies with given moments of inertia. The tethers consist of a number of finite cylindric beams or alternatively mass points. This feature provides a valuable way of evaluating the simulations results under two different approximations.

Considering the key questions above, our simulation produces both stable and unstable sail configurations depending on sail details. Presently, the most promising version is such that the auxiliary tethers are flexible and kept relatively tight during the flight. The deployment of the sail can be envisioned as a continuous sequence of self-similar stages from initial to the final stage. This has been simulated successfully including the remote unit thrusters generating the required angular momentum. Both during the flight and deployment, the main spacecraft and remote units can be followed. The sail details adopted for the ESAIL project are based on these simulation results. As an example, Figure 5 shows a snapshot of a simulation run with a loose tether leaving the system after a sudden tether breaking and consequent cut of the tether.

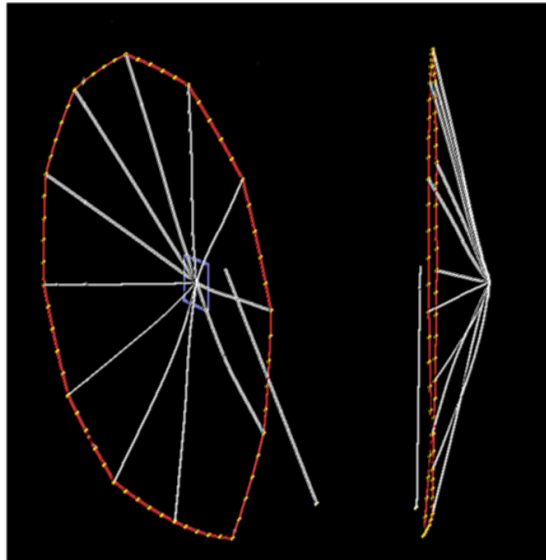


Figure 5. Fully dynamical simulation of main tether cut as seen from two viewing angles. In this case, at the time of the tether cut, thrusters at the main spacecraft are fired to produce impulsive 2.4 m/s delta-V in an attempt to pull the sail out of the way (to the right) of the cut tether leaving the system.

Rigid body model

Despite their limitations, rigid body simulations serves as tools for testing various control algorithms and developings flight algorithm for the electric sail. Since the fully dynamical simulation is computationally tedious, we also run a rigid body model. Flight simulations of the fully dynamical model suggest that a rigid model with a variable coning angle capture most of the sail temporal evolution caused by the solar wind variations. In reality, the rim of the sail can be expected to undulate and the main tethers to bend as shown by the dynamical simulation. The rigid body model is however expected to give an average behaviour of the sail to some extent. It is also a logical step between the fully dynamical simulation and the single tether model, and some of the analytical results of the single tether model can be deduced from the rigid body model. Most importantly, the rigid body simulation allows us to address the effects of the solar wind variations on the long term flight stability in statistical manner by evaluating the control schemes over the entire available solar wind data set. This supports also the design of the sail power system to optimize the thrust over the solar wind density data.

The rigid body of our simulation consists of a given number of rigid main tethers, remote units, and auxiliary tethers. These are defined by their moments of inertia. For the auxiliary tethers, we assume a minimum ring defined by the sail coning angle. Since the coning angle is allowed to vary in time, the total moments of inertia of the entire sail exhibit also temporal evolution. To couple the temporal evolution of the coning angle to the solar wind dynamic pressure, the model assumes presently slow temporal variations in the coning angle relative to the sail rotation. The coning angle is then defined in such a way that the solar wind push to the sail tethers is in balance with the opposing component of the centrifugal force.

SOLAR WIND VARIATIONS

Solar wind characteristics

Solar wind is tenuous fast flowing supersonic and super-Alfvénic plasma consisting mainly of protons and electrons. On the average, the plasma number density is 6.9 cm^{-3} , and the flow speed is 450 km/s. These values are computed from the OMNI data set⁶ that is available at <http://omniweb.gsfc.nasa.gov>. Figure 6a shows the solar wind number density and speed distribution for the entire OMNI data set. This implies that the sail attitude control and navigation have to handle wide ranges of both the density and speed values. Especially, as shown in Figure 6b, there are also considerable long term density variations that are issues for the navigation and associated design of the sail power system.

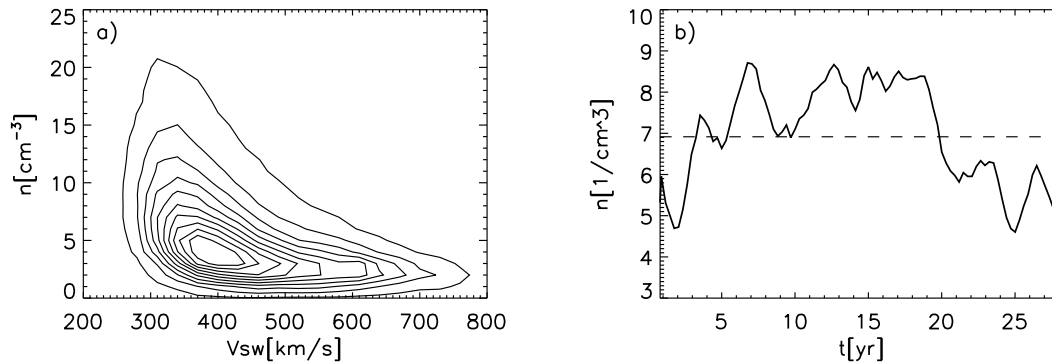


Figure 6. a) Distribution of solar wind density and speed and b) running average of the solar wind density over the data set.

Concerning the sail attitude control, the central feature of the solar wind is the velocity components perpendicular to the nominal radial wind direction. The distribution of these components are shown in Figure 7. These components can be expected to form a natural source for disturbances in azimuthal directions and cause phase drift of the tether if the auxiliary tethers are not used. This is especially the case since the time scale of the temporal variation of these components can be shorter than the sail rotation period leading to differential disturbances depending on the tether rotation phase.

Single tether control

The attitude control of a single tether under varying solar wind conditions is a central issue of the original sail design with mechanically separate tethers. This includes control over both the sail angle and tether rotation rate and phase. However, there is only one control parameter, the tether voltage for the single tether control, and controlling motion with two degrees of freedom is in principle an ill-posed problem. Since the radial dimensions of any spacecraft are negligible when compared to typical tether lengths, the azimuthal tether motion is not centrifugally stabilized by the finite central plate effect as is the case with the helicopter blades. Thus any disturbance to the tether spin rate leaves the tether phases to drift and ultimately leads to colliding tethers if not controlled.

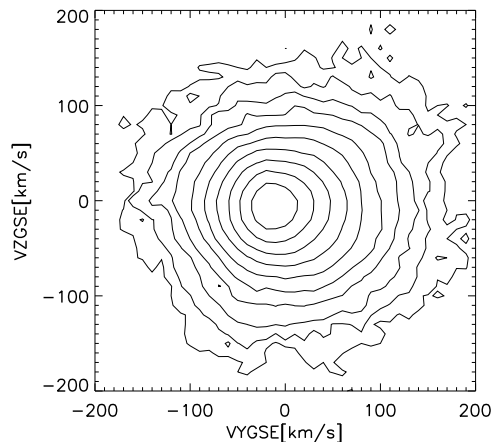


Figure 7. Distribution of non-radial solar wind components.

As shown in Figure 4, the tether spin rate depends on the sail turning angle. This effect allows us to control the tether spin rate by changing the sail angle. Figure 8 shows the tether rotation phase and sail angle as functions of time under varying solar wind conditions. The sail tether locations can then be expected to vary in an angular cone of about $\pm 5^\circ$ in phase and sail angle. Such a large angular cone limits the number of the tethers in the sail. The cone can be made smaller, in principle by increasing the sail spin rate, but considering mission time scales tethers may well drift out of the accepted cone and ultimately cause severe problems for the sail as whole. This motivates the design with mechanical stability relying on the auxiliary tethers.

Rigid body control

Collectively, there are effectively three control parameters left in the rigid body model when the total solar wind torque to the sail is summed over the given number of the main tethers. The controlling tether modulation can be given as

$$g(\varphi) = g_0 + g_1 \cos(\varphi) + g_2 \sin(\varphi), \quad (4)$$

where g_0 is the “throttle” while g_1 and g_2 provide control over the sail angle and phase. Figure 9 shows temporal evolution of these control parameters and the sail parameters, sail phase, sail angle, and coning angle under varying solar wind conditions.

The number of the control parameters imply that the sail rotation rate cannot be independently controlled. However, the relative variations to the spin rate caused by the non-radial solar wind components are small and causes statistically no problem. Concerning the Coriolis effect, predicted by the single tether model, the effect of these wind components may well be used to compensate the undesired spin rate evolution while orbiting around the Sun by introducing a clever control routine.

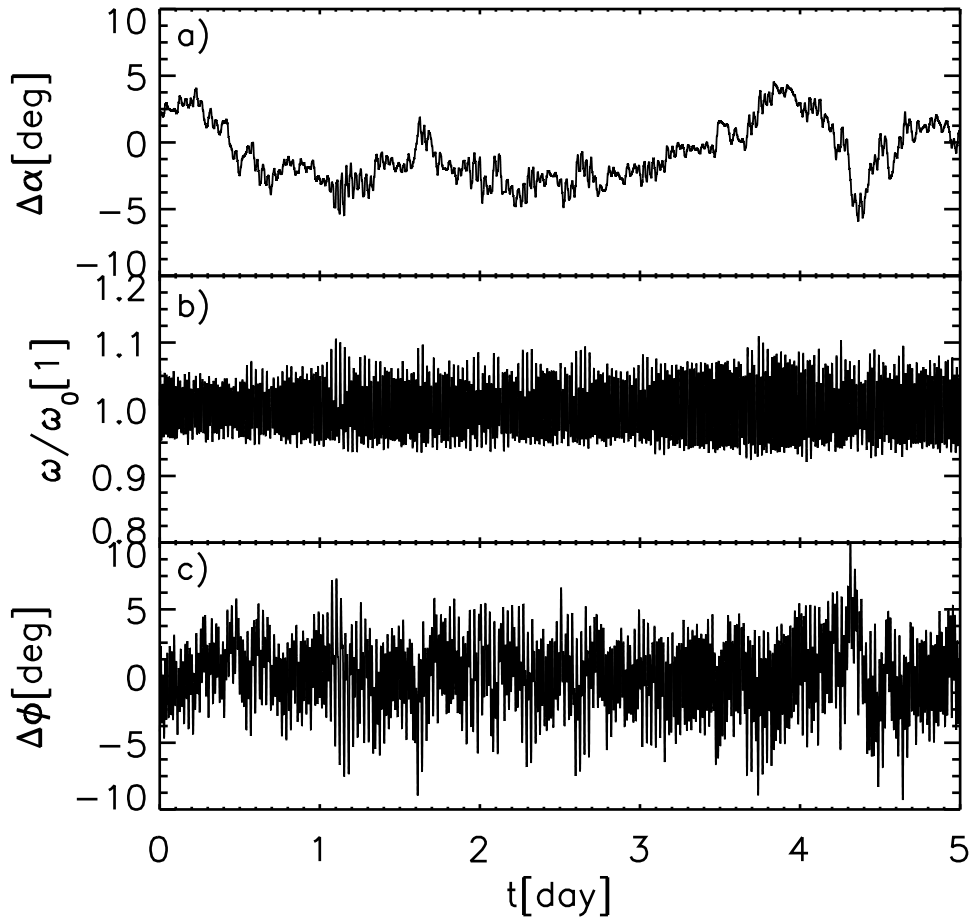


Figure 8. Five days of simulated single tether dynamics under variable solar wind conditions: a) differential sail angle, b) relative angular frequency, and c) differential sail rotation phase. The initial sail angle is 45° .

Navigation

Given the sail attitude control, the sail navigation can be addressed under variable solar wind conditions. As shown by,⁹ the electric sail can be navigated to planetary objects. Using an optimal transfer orbit to Mars⁷ as a mission plan, it was concluded that even with a relatively simple navigation control, accurate approach to Mars can be provided even under varying solar wind conditions. The navigation scheme was based only on an onboard accelerometer and a simple control of monitoring the integrated orbital speed against the planned speed. Launching a number of test spacecraft with random launch dates, it was shown that the conclusions are valid also in statistical sense. As a feasibility study, the navigation system can be extended by other tracking systems such as sun and star sensors for enhanced navigation accuracy.

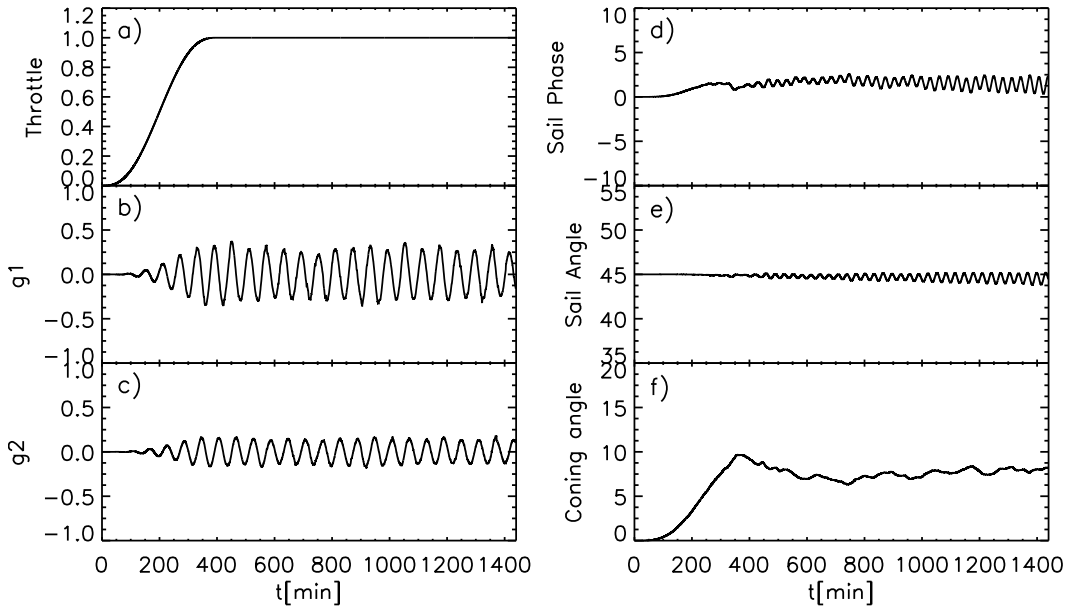


Figure 9. Output of rigid body simulation

CONCLUSION

In this paper, we reviewed the present status of the electric sail attitude and navigation control. We described three dynamical models developed for this purpose, a single tether model, a rigid body model, and a fully dynamical model. Using the single tether model, analytical expressions for the key sail parameters can be deduced, especially, the fraction of power to be reserved for the sail control can be obtained, and the enhancement of the sail rotation rate while turning the sail was presented. Furthermore, as implied by the latter result, the rotation rate temporal evolution while orbiting around the Sun was predicted and an expression for the magnitude of this effect was presented. The rigid body model can then be seen as an intermediate between the single tether model and the fully dynamical model. This model assumes the present version of the sail design including the remote units and auxiliary tethers. Some of the analytical results of the single tether model can also be derived for the rigid body model as a future study. The main difference of these models is that the azimuthal speed of the single tether varies over the rotation phase and more control power is required whereas with the auxiliary tethers the tether speeds are equal. The fully dynamical model then gives a full description of the sail dynamics including flexible tethers and mechanical interactions of the tethers, the main spacecraft, and the remote units described by their given moments of inertia. This simulation is the best tool to study the deployment and flight dynamics of the sail in details.

The solar wind characteristics have to be taken into account when designing the sail power system, attitude control, and navigation. The amount of electric current collected by the charged main tethers and the solar panel power required depends on the solar wind electron number density. Thus designing the power system is a tradeoff between the power system mass and the range of densities typical for the solar wind. The development of the

sail attitude control is a work in progress. Here, we described the solar wind characteristics central to the sail control as predicted by the actual solar wind data. It was shown that the control of single tether rotation phase can be based on the tether rotation rate dependence on the sail angle. However, this is most probably only the case for time periods of days, and for mission time scales, additional method of controlling both rotation phase and sail angle independently should be accomplished. The use of auxiliary tethers makes the sail mechanically stable as predicted by the full dynamical simulations. Since this simulation is computationally tedious, we are using the rigid body simulation to address the long-term effects of solar wind variations to the sail control. An important issue to be addressed using this model is that to what extent the Coriolis effect associated with the orbiting around the Sun can be reduced by using the non-radial solar wind components. The key components of the electric sail are being developed in an EU/FP7 ESAIL project. These components and their specifications were identified based on our fully dynamical simulation.

ACKNOWLEDGEMENTS

This research was financed within the European Community's Seventh Framework Programme ([FP7/2007-2013]) under grant agreement number 262733 and the Academy of Finland grant decision 250591. This work was also supported by Academy of Finland. The OMNI data were obtained from the GSFC/SPDF OMNIWeb interface.

REFERENCES

- [1] R. Hoyt and R. L. Forward, "Alternate interconnection Hoytether failure resistant multiline tether," U.S. Patent No. 6,286,788 B1, 2001.
- [2] P. Janhunen, "Electric sail for spacecraft propulsion," *J. Propul. Power*, Vol. 20, pp. 763–764, 2004.
- [3] P. Janhunen and A. Sandroos, "Simulation study of solar wind push on a charged wire: basis of solar wind electric sail propulsion," *Ann. Geophys.*, Vol. 25, pp. 755–767, 2007.
- [4] P. Janhunen, "Electric sail for producing spacecraft propulsion," U.S. Patent No. 7,641,151, 2010.
- [5] P. Janhunen, P. K. Toivanen, J. Polkko, S. Merikallio, P. Salminen, E. Haegström, H. Seppänen, R. Kurppa, J. Ukkonen, S. Kiprich, G. Thornell, H. Kratz, L. Richter, O. Krömer, R. Rosta, M. Noorma, J. Envall, S. Lätt, G. Mengali, A. A. Quarta, H. Koivisto, O. Tarvainen, T. Kalvas, J. Kauppinen, A. Nuottajärvi, and A. Obraztsov, "Electric solar wind sail: Towards test missions," *Rev. Sci. Instrum.*, Vol. 81, 111301, 2010.
- [6] J. H. King and N. E. Papitashvili, "Solar wind spatial scales in and comparisons of hourly Wind and ACE plasma and magnetic field data," *J. Geophys. Res.*, 110, A02104, doi:10.1029/2004JA010649, 2004.
- [7] G. Mengali, A. A. Quarta, and P. Janhunen, "Electric sail performance analysis," *J. Spacecraft Rockets*, 45, pp. 122–129, 2008.
- [8] J. R. Sanmartín, E. Chroinière, B. E. Gilchrist, J.-B. Ferry, and M. Martínez-Sánchez, "Bare-tether sheath and current: comparison of asymptotic theory and kinetic simulations in stationary plasma," *IEEE Trans. Plasma Phys.*, Vol. 36, pp. 2851–2858, 2008.
- [9] P. K. Toivanen and P. Janhunen, "Electric sailing under observed solar wind conditions," *Astrophys. Space Sci. Trans.*, Vol. 5, pp. 61–69, 2009.
- [10] P. K. Toivanen and P. Janhunen, "Spin plane control and thrust vectoring of electric solar wind sail by tether potential modulation," *J. Propul. Power*, Submitted, 2012.
- [11] R. M. Zubrin and D. G. Andrews, "Magnetic sails and interplanetary travel," *J. Spacecraft Rockets*, Vol. 28, pp. 197–203, 1991.